

Simulation and optimization of GaAs_{1-x}P_x/Si_{1-y}Ge_y/Ge triple junction solar cells

A. B. Azzououm^b, A. Aissat^{a,b,c*}, J. P. Vilcot^c

^aUniversity of Ahmed Draya, Adrar, Algeria

^bFaculty of Technology, University of Blida.1, Algeria

^cInstitute of Microelectronics, Electronics and Nanotechnology (IEMN), UMR CNRS 8520. University of Sciences and Technologies of Lille 1. Poincare Avenue, 60069, 59652 Villeneuve of Ascq, France

This paper focuses on studying and simulating a GaAs_{1-x}P_x/Si_{1-y}Ge_y/Ge triple-junction solar cell structure. First, the strain and the bandgap energy associated to the SiGe layer have been studied. The optimal germanium concentration is 0.88 with a strain around 0.45%. Then, the phosphor concentration effect on the strain and the bandgap energy of the upper layer GaAs_{1-x}P_x/Si_{0.12}Ge_{0.88} has been optimized. At room temperature, the optimal output parameter reach $J_{sc}=34.41\text{mA/cm}^2$, $V_{oc}=1.27\text{V}$, $FF=88.42\%$ and $\eta=38.45\%$ for an absorber thickness of $4.5\mu\text{m}$ and $x=0.47$, with a strain that doesn't exceed 1.5%. This study has enabled us to design a high-efficiency, low cost 3J solar cell.

(Received October 23, 2023; Accepted January 13, 2024)

Keywords: Semiconductors, Efficiency, Triple junction, Solar cell, Photovoltaic

1. Introduction

Increasing the efficiency of a solar cell leads to the diminution of watt peak cost [1]. Among the technologies offering a boost in efficiency, we find the multijunction solar cell. This latter is based on the stacking of a set of semiconductor materials with different bandgap energies, this arrangement aims to absorb the maximum of the solar spectrum [2].

In fact, the multijunction solar cell based on III-V compound materials presents higher efficiency and seem to be the future for photovoltaics applications. More and more, they have become the most prospective space solar technology [3,4]. However, the fabrication cost of these configurations still expensive. One of the techniques employed to reduce the cost is the use of the silicon substrate. Therefore, monolithically grown GaAsP/Si cells may be a suitable candidate to supply low cost and high efficiency solar power for space applications.

Although, it is known that in experiments there is a difficulty to grow III-V materials with silicon due to the high lattice mismatch and the large difference in thermal expansion coefficients [5-8]. A promising way to surmount these limitations and increase the III-V 3J solar cells efficiency of consists in using the germanium element as a bottom cell instead of silicon. The germanium is characterized by direct bandgap energy of 0.66 eV at 300K, so the absorption edge is steeper than Si, a greater spectral overlap of the solar irradiance spectrum and low cost materials. Besides, the germanium element can be grown with lattice match to III-V materials. This superiority of germanium makes it a promising material to absorb low energy photons [9,10]. For these last reasons, in the present work, germanium is adopted as a bottom cell.

The integration of SiGe as a buffer layer between the III-V top solar cell and bottom cell can reduce the dislocation interface for III-V nucleation and give high quality of bottom solar cell. Fadaly et al. [11] demonstrated that the calculated lifetimes of Si_{1-y}Ge_y alloys approach those of group III-V semiconductors because they are theoretically predicted to combine a direct bandgap, wavelength tenability and strong optical transitions [11-13].

Moreover, an experimental structure GaAs_{0.79}P_{0.21}/Si_{0.18}Ge_{0.82} double junction solar cell was elaborated as reported in [12]. In the goal to enhance their performances, a triple junction was

*Corresponding author: sakre23@yahoo.fr
<https://doi.org/10.15251/JOR.2024.201.75>

modeled and proposed in the present work. A simulation of optical and electrical properties such as current density voltage (J-V), the external quantum efficiency (EQE) and photoluminescence spectra (PL) were performed to optimize this 3J solar cell through studying the influence of base top solar cell phosphorus composition. Figure 1 presents the adopted structure, which summarizes the parameters used along this simulation. This 3J solar cell consists of three solar cells arranged as follow: top solar cell made of GaAsP, middle solar cell made of SiGe and a bottom solar cell made of Ge. Two highly doped tunnel junctions: p-GaAs/n-Si and p-Ge/n-Ge are placed between the top/middle cell and the middle/bottom solar cell, respectively.

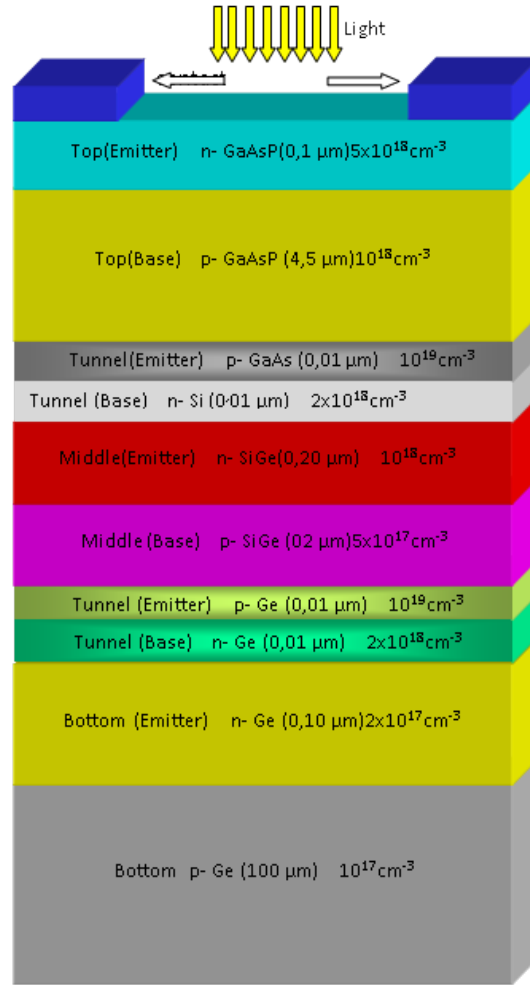


Fig. 1. Structure of $GaAs_{1-x}P_x/Si_{0.12}Ge_{0.88}/Ge$ triple junctions solar cell [12].

2. Theoretical model

The carrier recombination modeled by Shockley Read Hall (SRH) recombination using a concentration dependent lifetime model and the mobility of carrier dependent concentration described by Masetti model are given in detail in [14]. The Drift-Diffusion model is used to calculate the current density of electrons and holes; the Poisson equations are given by [15,16]. The expression of EQE is given by [17]:

$$J_{ph} = q \int_{\lambda_i}^{\lambda_f} F(\lambda) \cdot EQE(\lambda) d\lambda \quad (1)$$

Where J_{ph} is the photocurrent supplied by the solar cell; $F(\lambda)$ is spectral solar irradiance; λ_i is initial wavelength and λ_f is the final wavelength.

The bandgap energy of $\text{GaAs}_{1-x}\text{P}_x$ is written as [18]:

$$E_{g \text{ GaAs}_{1-x}\text{P}_x} = E_{g \text{ GaAs}} \cdot (1 - x) + E_{g \text{ GaP}} \cdot x - b \cdot x \cdot (1 - x) \quad (2)$$

where $E_{g \text{ GaAs}}$ and $E_{g \text{ GaP}}$ are the bandgap energies of GaAs and GaP at room temperature respectively. The bandgap energies of GaAs and GaP are 1.42 and 2.26 eV [19], respectively, b is the Bowing parameter of $\text{GaAs}_{1-x}\text{P}_x$ ($b= 0.1\text{eV}$). The unstrained bandgap energy of $\text{Si}_{1-y}\text{Ge}_y$ structure is given by [20]:

$$E_{g \text{ (SiGe)}}(y) = \begin{cases} 1.17 - 0.47y + 0.24y^2, & y < 85 \\ 5.88 - 9.58y + 4.43y^2, & y \geq 85 \end{cases} \quad (3)$$

While, the strained bandgap energy of $\text{Si}_{1-y}\text{Ge}_y$ structure is given by [20]:

$$E_{g \text{ (SiGe)}}(y) = 1.17 - 0.94y + 0.34y^2 \quad (4)$$

The lattice parameter of the ternary material $\text{GaAs}_{1-x}\text{P}_x$ as function of the x composition is calculated by using the Vegard's law:

$$a_{\text{GaAs}_{1-x}\text{P}_x} = a_{\text{GaAs}} \cdot (1 - x) + a_{\text{GaP}} \cdot x \quad (5)$$

Where a_{GaAsP} , a_{GaAs} and a_{GaP} are respectively the lattice constant of GaAsP, GaAs and GaP, they are given as: $a_{\text{GaAs}} = 5.65 \text{ \AA}$ and $a_{\text{GaP}} = 5.45 \text{ \AA}$ [21].

The strain produced between $\text{Si}_{1-y}\text{Ge}_y$ and Ge is given by:

$$\varepsilon_2 = \frac{a_{\text{Ge}} - a_{\text{Si}_{1-y}\text{Ge}_y}}{a_{\text{Si}_{1-y}\text{Ge}_y}} \quad (6)$$

with a_{Ge} is 5.66 \AA [21].

The strain produced between $\text{GaAs}_{1-x}\text{P}_x$ and $\text{Si}_{0.12}\text{Ge}_{0.88}$ is defined as:

$$\varepsilon_1 = \frac{a_{\text{Si}_{0.12}\text{Ge}_{0.88}} - a_{\text{GaAs}_{1-x}\text{P}_x}}{a_{\text{GaAs}_{1-x}\text{P}_x}} \quad (7)$$

with $a_{\text{Si}_{0.12}\text{Ge}_{0.88}}$ is 5.63 \AA .

The physical and optical parameters of materials used along this simulation are taken from [15,16,22] and summarizes in Table 1.

Table 1. The parameters of the materials used in the simulation.

	GaAs	GaP	$\text{Si}_{0.12}\text{Ge}_{0.88}$
E_g (eV)	1.42	2.26	0.82
ε_r	13.1	11.10	15.5
χ_e (eV)	4.07	4.4	4.17
a (Å)	5.65	5.45	5.63
N_C ($1/\text{cm}^3$)	$4.7 \cdot 10^{17}$	$1.76 \cdot 10^{18}$	$1.25 \cdot 10^{19}$
N_V ($1/\text{cm}^3$)	$7 \cdot 10^{18}$	$8.87 \cdot 10^{18}$	$0.65 \cdot 10^{19}$

3. Results and discussion

In these parts of the work, numerical simulations have been carried out at room temperature under the AM_0 solar spectrum with a light source at normal incidence. In order to improve the performance of the proposed solar cell based on $GaAs_{1-x}P_x/Si_{0.12}Ge_{0.88}/Ge$ materials, the phosphorus concentration (P) effect of the basic top cell is investigated. In this simulation, the drift diffusion and Poisson equations described in [15,16] are coupled and solved numerically to present and discuss the important characteristic J-V parameters and external quantum efficiency (EQE) of this exposed solar cell. After that, we simulated the structure of the triple-junction solar cell. The J-V and EQE characteristics were compared with experimental tandem solar cells.

Figure 2 shows the variation in strain between the layers formed by the $Si_{1-y}Ge_y$ and Ge materials. It also shows the impact of the germanium concentration (y) on the bandgap energy in the unstrained and strained cases. The results for the unstrained bandgap energy were validated by experimental results from ref [23-25]. We note that the experimental results are in very good agreement with the simulation. The blue-sky curve shows the bandgap energy of SiGe in the strained case. When the Ge concentration varies from 0 to 1, the strained bandgap energy varies from 1.12 to 0.67eV. This simulation allows us to optimize the y concentration. After this simulation we were able to take up y equal 0.88, i.e. $E_g=0.95eV$. The red curve illustrates the influence of the concentration y on the strain ϵ . For $y=0.88$ the strain does not exceed 0.45%. The structure $Si_{0.12}Ge_{0.88}/Ge$ is consequently stable.

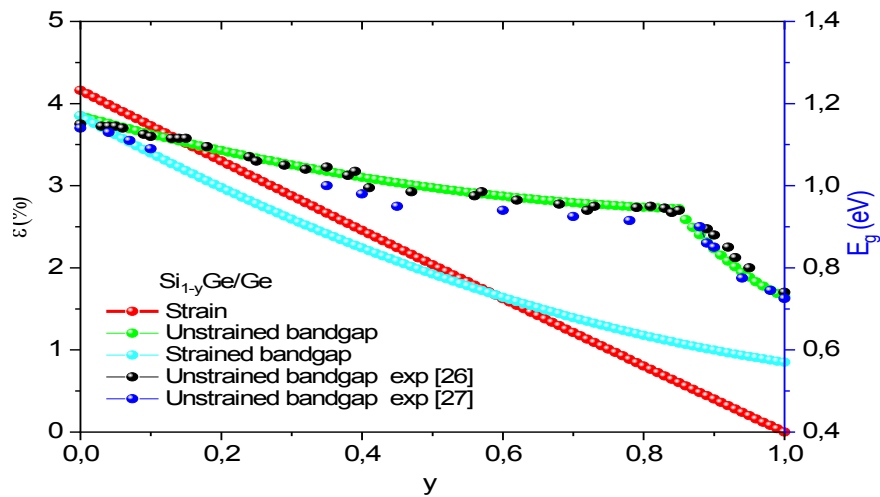


Fig. 2. Strain and bandgap energy of $Si_{1-y}Ge_y/Ge$ as function of Germanium composition [26,27].

Figure 3 shows the phosphorus concentration (x) effect on the strain between the two layers $GaAsP$ and $Si_{0.12}Ge_{0.88}$. Also, the influence of the concentration x on the unstrained and strained bandgap energy has also been simulated. When the concentration x changes from 0 to 1 the bandgap energy increases from 1.17 to 2.7eV. This simulation allows us to optimize the bandgap energy of the top solar cell structure ($GaAsP$). Besides, the unstrained bandgap energy ($\epsilon=0$) has been validated by experimental results presented by H. Soon et al [26]. Our simulation results are in accord with the experimental results. This simulation allows us to optimize the concentration x in order to minimize the deformation. For example, for $x=0.47$ the deformation does not exceed 1.5%. This stress value is acceptable for making a sand structure. For a strain of 1.5% the bandgap energy of the $GaAsP$ absorber is around 1.55eV. Figure 4 shows the variation of the external quantum efficiency as a function of wavelength. The characteristic parameters of this structure are listed in table 2. We observe that the absorption range of the proposed structure varies from 225 to 900nm with the amplitude of $EQE=90\%$. These results were validated by two other measured results from refs [27] and [28]. We notice that the absorption range obtained by [27,28] varies from 300 to 778 nm. The absorption range of our structure is larger than the absorption range found by refs [27,28]. So we got a relative absorption gain of 29.12%.

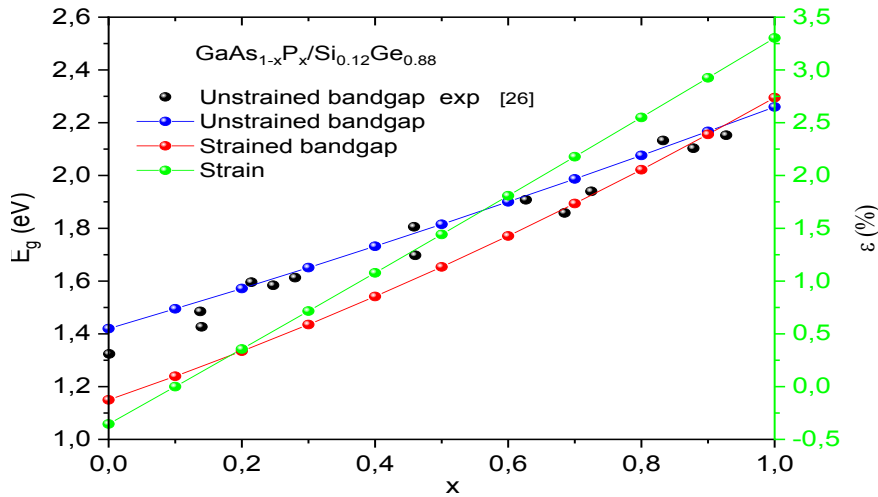


Fig. 3. Strain and bandgap energy of $\text{GaAs}_{1-x}\text{P}_x/\text{Si}_{0.12}\text{Ge}_{0.88}$ as function of Phosphorus composition [27].

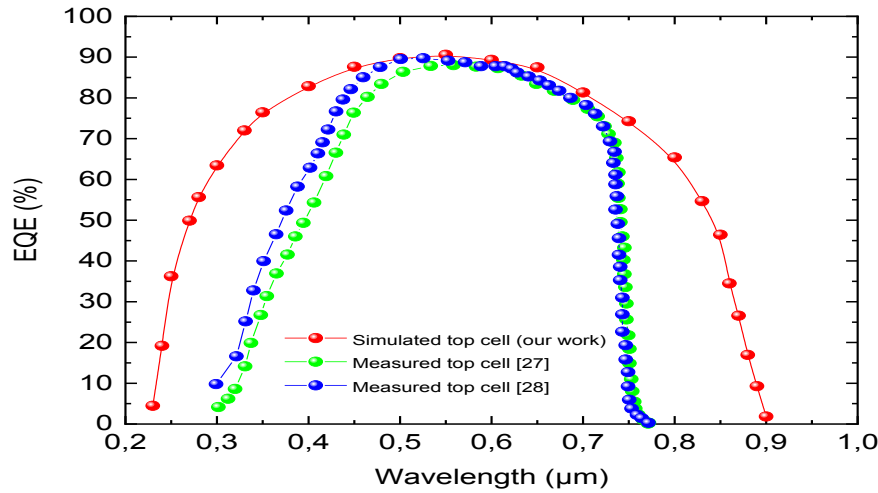


Fig. 4. EQE spectrum of both simulated GaAsP top sub-cell and experimental GaAsP top sub-cell [27,28].

Table 2. Electrical parameters of triple solar cell with various phosphorus compositions.

x	0.17	0.27	0.37	0.47	0.57
$J_{SC}(\text{mA}/\text{cm}^2)$	36.41	35.88	35.25	34.41	33.23
$V_{OC}(\text{V})$	1.06	1.13	1.21	1.27	1.24
FF (%)	87.47	87.99	88.22	88.42	87.58
Efficiency(%)	33.89	35.81	37.64	38.45	36.10

Figure 5 shows the variation of the current density of three single solar cells and the total solar cell as a function of voltage. The results show that the open circuit voltage reaches 1.27V and the short circuit current density is around $35\text{mA}/\text{cm}^2$. The proposed optimized solar cell efficiency exceeds 38% for $x=0.47$, $y=0.88$ with $\epsilon_{\text{SiGe}/\text{Ge}}=0.45\%$ and $\epsilon_{\text{GaAsP}/\text{SiGe}}=1.5\%$. For a concentration $x=0.57$ the efficiency begins to decrease and is equal to 36.10%. This degradation due to increase in strain which exceeds 1.75%.

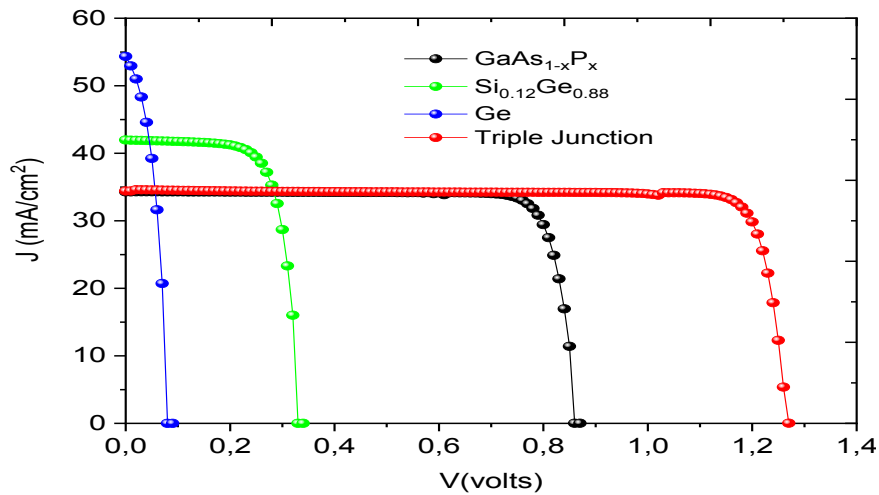


Fig. 5. J - V curve of the triple junction solar cell and the individual solar cells.

The effect of phosphorus concentration on the 3J solar cell parameters, (short circuit current density and open circuit voltage) was also investigated. Figure 6 shows the J - V characteristic of the proposed solar cell for different phosphorus concentrations. We notice that J_{sc} and V_{oc} change with increasing phosphorus concentration. When changing x from 0.17 to 0.47 with $d=4.5\mu\text{m}$, the density J_{sc} decreases and the voltage V_{oc} increases. The decrease in J_{sc} is $\Delta J_{sc}=3.7\text{mA}/\text{cm}^2$ and the gain in V_{oc} is around 0.21V, with a strain that doesn't exceed 1.25%. Based to the table 3, we note that when we increase the thickness, the efficiency is boosting until it gets a maximum of about 38.45 % at a thickness of 4.5 μm .

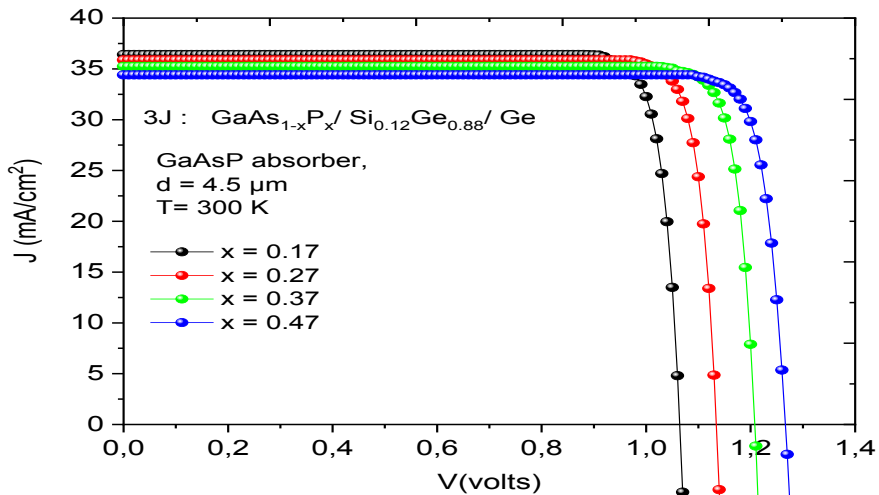


Fig. 6. J - V of triple junction solar cell for different P concentration.

Table 3. Electrical parameters of triple solar cell with various base $\text{GaAs}_{1-x}\text{P}_x$ absorber thicknesses.

GaAsP absorber Thickness (μm)	1.5	3	4,5	6	7,5
$J_{sc}(\text{mA}/\text{cm}^2)$	28.58	32.52	34.41	39.53	36.27
$V_{oc}(\text{V})$	1.24	1.26	1.27	1.27	1.28
FF (%)	87.48	88.09	88.42	88.22	88.19
η (%)	30.92	35.97	38.45	39.92	40.91

Figure 7 illustrates the power variation of the proposed solar cell as a function of voltage for different phosphorus concentrations. Increasing the phosphorus concentration causes a significant increase in the maximum output power density. When varying phosphorus concentration from 0.17 to 0.47, the maximum power density changes from 32mW/cm² to 37.20mW/cm², that is to say we have a gain of $\Delta g=5.2\text{mW/cm}^2$.

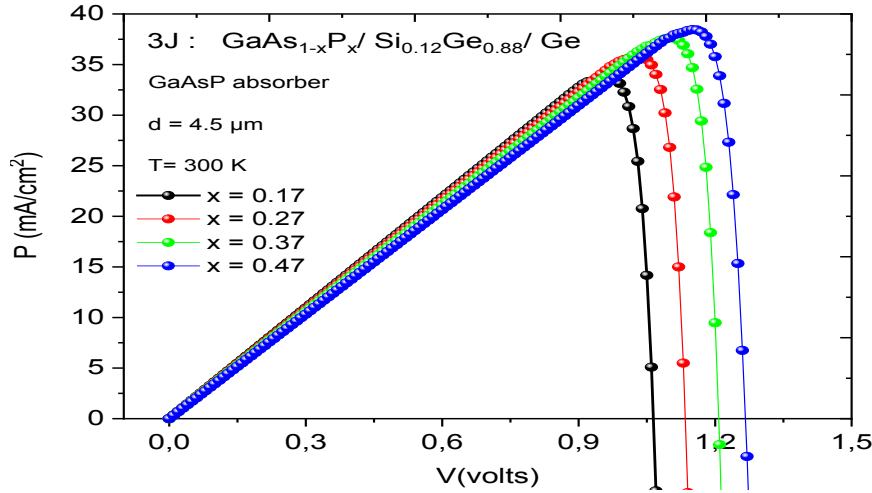


Fig. 7. *P-V of triple junction solar cell for different P concentration.*

Figure 8 shows the effect of the GaAsP structure absorber thickness (d) on the total solar cell (3J) output parameters J_{sc} , V_{oc} , FF and η . Figure 8.a illustrates the variation of J_{sc} and V_{oc} as a function of the $\text{GaAs}_{1-x}\text{P}_x$ absorber thickness for $x=0.47$ with $\epsilon=1.25\%$.

We note that increasing the thickness d from 1.5 to $6\mu\text{m}$ induces a considerable increase in J_{sc} from 28 to 39mA/cm^2 , i.e. a gain of 11mA/cm^2 . While, the variation of the thickness has a small effect on V_{oc} with a gain of around 0.026V is obtained.

For the same phosphor content and the same strain as in Figure 8.a, the effect of the $\text{GaAs}_{1-x}\text{P}_x$ absorber thickness d on the 3J solar cell FF and efficiency is illustrated in Figure 8. b. As increasing GaAsP absorber thickness, a positive change is imposed on both parameters FF and η . When changing the thickness from 1.5 to $6\mu\text{m}$, the FF varies from 87.48 to 88.22%, which represents an increase of 0.74%. In addition, we find that the efficiency increases rapidly from 30.92 to 39.92%, i.e. a gain of 9%. Based on this investigation, the optimal efficiency of the proposed solar cell corresponds to $x=0.47$, $\epsilon=1.25\%$, $d=4.5\mu\text{m}$ and $y=0.88$. Under these conditions, the output parameters reach: $J_{sc}=34.41\text{mA/cm}^2$, $V_{oc}=1.27\text{V}$, $\text{FF}=88.42\%$ and $\eta=38.45\%$.

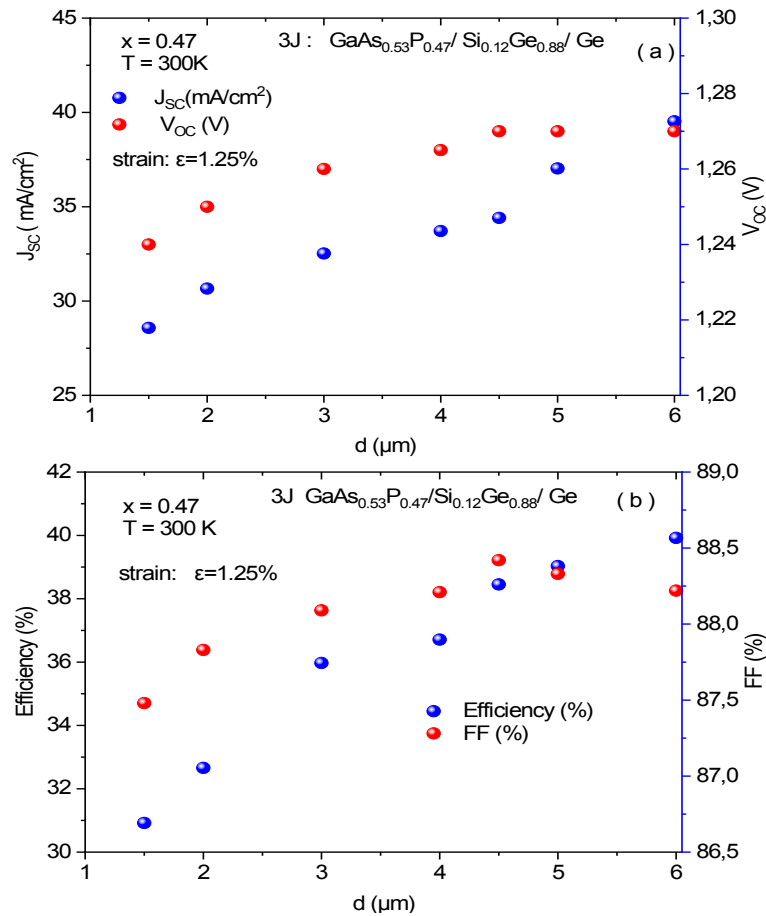


Fig. 8 (a,b). Variations of the proposed solar cell output parameters as a function of the thickness d of the GaAsP absorber layer, a) Effect of d on the J_{sc} and V_{oc} , b) Effect of d on the FF and η .

Figure 9 provides a comparison of a double-junction solar cell proposed by K. J. Schmieder et al. [12] and Martin Diaz et al. [27] with the present work results concerning the $\text{GaAs}_{0.53}\text{P}_{0.47}/\text{Si}_{0.12}\text{Ge}_{0.88}/\text{Ge}$ solar cell for $d=1.5\mu\text{m}$. It can be noticed that the proposed 2J solar cell in [12] has an efficiency of 15%. Also, the solar cell in [27] presents experimental and calculated efficiencies of 17.80% and 18.90% respectively. Whereas, with a thickness of $d=1.5\mu\text{m}$, our proposed solar cell, which is based on $\text{GaAs}_{0.53}\text{P}_{0.47}/\text{Si}_{0.12}\text{Ge}_{0.88}/\text{Ge}$, exhibits a better efficiency of about 30.92%.

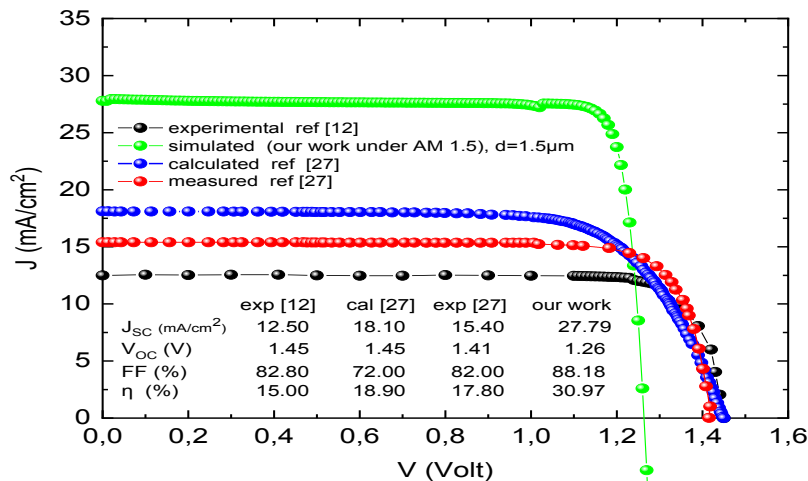


Fig. 9. J - V characteristic of both simulated triple junction solar cell ($d=1.5\mu\text{m}$) and experimental tandem solar cells [12,27].

4. Conclusion

In the present work, a novel structure of GaAs_{1-x}P_x/Si_{1-y}Ge_y/Ge triple junction solar cell has numerically simulated and optimized. The bandgap energy of the two layers SiGe and GaAsP has been optimized. The bandgap energies of the absorber layers are $E_g(y=0.88)=0.95\text{eV}$ and $E_g(x=0.47)=1.55\text{eV}$ respectively. For an upper cell absorber layer thickness of $d=4.5\mu\text{m}$ and a phosphorus composition at $x=0.47$, the optimum efficiency is around 38.45% with $\epsilon_{\text{SiGe/Ge}}=0.45\%$ and $\epsilon_{\text{GaAsP/SiGe}}=1.5\%$. In the future, we aim to extend our research to solar cells based on new alloys, mainly quaternary and quinary alloys, to model and optimize 4- and 5-junction solar cells.

Acknowledgements

The authors would like to thank the Tempus Esience project team (Project n°:530341-TEMPUS-1-2012-1-FR-TEMPUS-JPCR from 2012 to 2015) for providing us with the virtual lab of the University of Bordj BouArreridj (UBBA vlab) and allowed us using the TCAD-Silvaco software to model and characterize our solar cells.

References

- [1] S. Essig, C. Allebé, T. Remo, J. F. Geisz, M. A. Steiner, K. Horowitz, L. Barraud, J. S. Ward, M. Schnabel, A. Descoedres, D. L. Young, M. Woodhouse, M. Despeisse, C. Ballif, Tamboli, *Nature energy* 2(9), 1(2017) ; <https://doi.org/10.1038/nenergy.2017.144>
- [2] M. Yamaguchi, K. H. Lee, K. Araki, N. Kojima, *J. Phys. D: Applied physics* 51(13), 133002(2018) ; <https://doi.org/10.1088/1361-6463/aaaf08>
- [3] R. Cariou, W. Chen, G. Hamon, M. Foldyna, R. Lachaume, J. Alvarez, J.-L. Maurice, J. Decobert, J.-P. Kleider, P. Roca Cabarrocas International Conference on the Formation of Semiconductor Interfaces 17, (2015).
- [4] S. Bernardes, R.A.M Lameirinhas, J.N. Torres, C.A.F. Fernandes, *Nanomaterials* 11(1), 1(2021) ; <https://doi.org/10.3390/nano11010078>
- [5] R. Lachaume, R. Cariou, J. Decobert, M. Foldyna, G. Hamon, P.R iCabarrocas, J. Alvarez, J.-P. Kleider, *Energy Procedia* 84, 41(2015) ; <https://doi.org/10.1016/j.egypro.2015.12.293>
- [6] J.P. Connolly, D. Mencaraglia, C. Renard, D. Bouchier, *Prog. Photovolt. Res. Appl.* 22(7), 810(2014) ; <https://doi.org/10.1002/ppp.2463>
- [7] M.A. Green, *Proc. SPIE 8981, Physics, Simulation, Photonic Engineering of Photovoltaic Devices III 8981*, 88(2014).
- [8] A. Bahi, A. Azzououm, A. Aissat, F. Benyettou, J.P. Vilcot, International Conference on Communications and Electrical Engineering (ICCEE), IEEE, 1(2018).
- [9] T. Masuda, J. Faucher, M.L. Lee, *Journal of Physics D: Applied Physics* 49(46), 1(2016) ; <https://doi.org/10.1088/0022-3727/49/46/465105>
- [10] G. Sun, F. Chang, R.A. Soref, *Optics express* 18(4), 3746 (2010) ; <https://doi.org/10.1364/OE.18.003746>
- [11] E. M.T. Fadaly, A. Dijkstra, J.R. Suckert, D. Ziss, M.A.J. van Tilburg, C. Mao, Y. Ren, V.T. van Lange, K. Korzun, S. Kölling, M.A. Verheijen, D. Busse, C. Rödl, J. Furthmüller, F. Bechstedt, J. Stang, J.J. Finley, S. Botti, J.E.M. Haverkort, E.P.A.M. Bakkers, *Nature* 580(7802), 205(2020) ; <https://doi.org/10.1038/s41586-020-2150-y>
- [12] K.J. Schmieder, A. Gerger, M. Diaz, Z. Pulwin, M. Curtin, L. Wang, A. Lochtefeld, R.L. Opila, A. Barnett, *Journal of Materials Science in Semiconductor Processing* 39, 614(2015) ; <https://doi.org/10.1016/j.mssp.2015.05.058>
- [13] Y. Liu, M. Ahmadpour, J. Adam, J.K.-Hansen, H.G. Rubahn, M. Madsen, *IEEE Journal of Photovoltaics* 8(5), 1363(2018) ; <https://doi.org/10.1109/JPHOTOV.2018.2851308>

- [14] F. Benyettou, A. Aissat, M. Benamar, J.P. Vilcot, *Energy Procedia* 74, 139(2015) ;
<https://doi.org/10.1016/j.egypro.2015.07.535>
- [15] D. Munteanu, J.L. Autran, In: *Nanowires-Recent Advances*. IntechOpen, 2012. Chapter 15, 341(2012).
- [16] S.M. Ramey, R. Khoie, *IEEE Trans. Electron Devices* 50(5), 1179(2003) ;
<https://doi.org/10.1109/TED.2003.813475>
- [17] C.H. Chiu, S.Y. Kuo, M.H. Lo, C.C. Ke, T.C. Wang, Y.T. Lee, H.C. Kuo, T.C. Lu, S.C. Wang, *Journal of Applied Physics* 105(6), 1(2009) ;
<https://doi.org/10.1063/1.3083074>
- [18] C. Bosio, J.L. Stachli, M. Guzzi, G. Burri, R.A. Logan, *Phys Rev B* 38(5), 3263(1988) ;
<https://doi.org/10.1103/PhysRevB.38.3263>
- [19] I. Vurgaftman, J.R. Meyer, L.R. Ram-Mohan, *Journal of Applied Physics* 89(11), 5815(2001) ;
<https://doi.org/10.1063/1.1368156>
- [20] Y.M. Haddara, P. Ashburn, D.M. Bagnall, In: Kasap, S., Capper, P. (eds) *Springer Handbook of Electronic and Photonic Materials*. Springer Handbooks. Springer, Cham. (2017).
- [21] I. Vurgaftman, J.R. Meyer, *Journal of Applied Physics* 94(6), 3675(2003) ;
<https://doi.org/10.1063/1.1600519>
- [22] A. Sadao, "Properties of Group IV, III-V, and II-VI Semiconductors", John Wiley & Sons Ltd, England, (2005).
- [23] R. Braunstein, A.R. Moore, F. Herman., *Phys. Rev.* 109(3), 695(1958) ;
<https://doi.org/10.1103/PhysRev.109.695>
- [24] S. Krishnamurthy, A. Sher, A.-B. Chen, *Phys. Rev. B*, 33(2), 1026(1986).
- [25] J. Weber, M.I. Alonso, *Phys. Rev. B*, 40(8), 5683(1989) ;
<https://doi.org/10.1103/PhysRevB.40.5683>
- [26] H.S. Im, C.S. Jung, K. Park, D.M. Jang, Y.R. Lim, J. Park, B.J. *Phys. Chem. C* 118(8), 4546(2014) ; <https://doi.org/10.1021/jp500458j>
- [27] M. Diaz, L. Wang, D. Li, X. Zhao, B. Conrad, A. Soeriyadi, A. Gerger, A. Lochtefeld, C. Ebert, R. Opila, I.P. Wurfl, A. Barnett, *Solar Energy Materials and Solar Cells*, 143, 113(2015) ;
<https://doi.org/10.1016/j.solmat.2015.06.033>
- [28] L. Wang, D. Li, X. Zhao, B. Conrad, M. Diaz, A. Soeriyadi, A. Lochtefeld, A. Gerger, I.P. Wurfl, A. Barnett, *Phys. Status Solidi (RRL)-Rapid Research Letters*, 10(8), 596(2016) ;
<https://doi.org/10.1002/pssr.201600157>